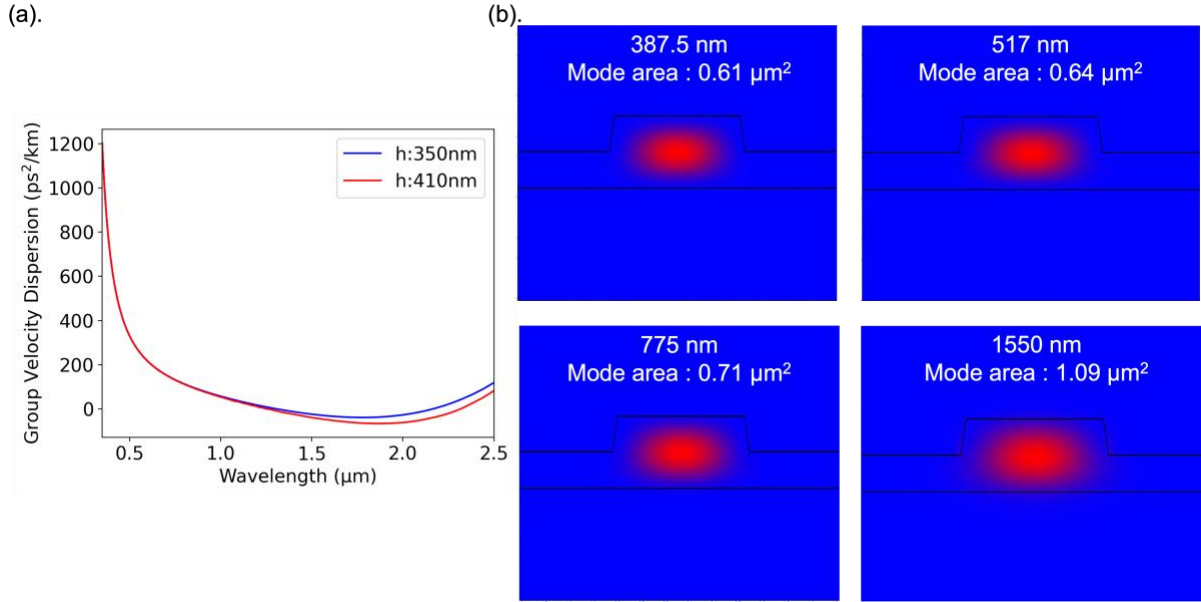


Visible-to-ultraviolet frequency comb generation in lithium niobate nanophotonic waveguides

In the format provided by the
authors and unedited

Supplementary Materials

Waveguide dispersion: In Supplemental Fig. 1(a), we present the calculated group velocity dispersion (GVD) for the waveguide used in this work, with $h=350$ nm. In this figure, h is the etch depth into the 700 nm film and the waveguide width is $w=1800$ nm. For comparison, a second waveguide is also shown with $h=410$ nm. For both waveguides in Fig. 1, the GVD is near zero at the pump wavelength of 1550 nm, and the GVD is strongly normal in the visible. Below wavelengths of 1000 nm, the impact of geometric dispersion engineering is negligible for these waveguides. In Supplemental Fig. 1(b), we show calculations of the TE mode profiles of different harmonic orders for the waveguide with $h=350$ nm. These calculations show that the fundamental TE₀₀ has good overlap with the lowest order confined modes of the higher-order harmonics. We also report the mode area at each wavelength, and see that it decreases from $1.09 \mu\text{m}^2$ at the fundamental to $0.61 \mu\text{m}^2$ in the UV.



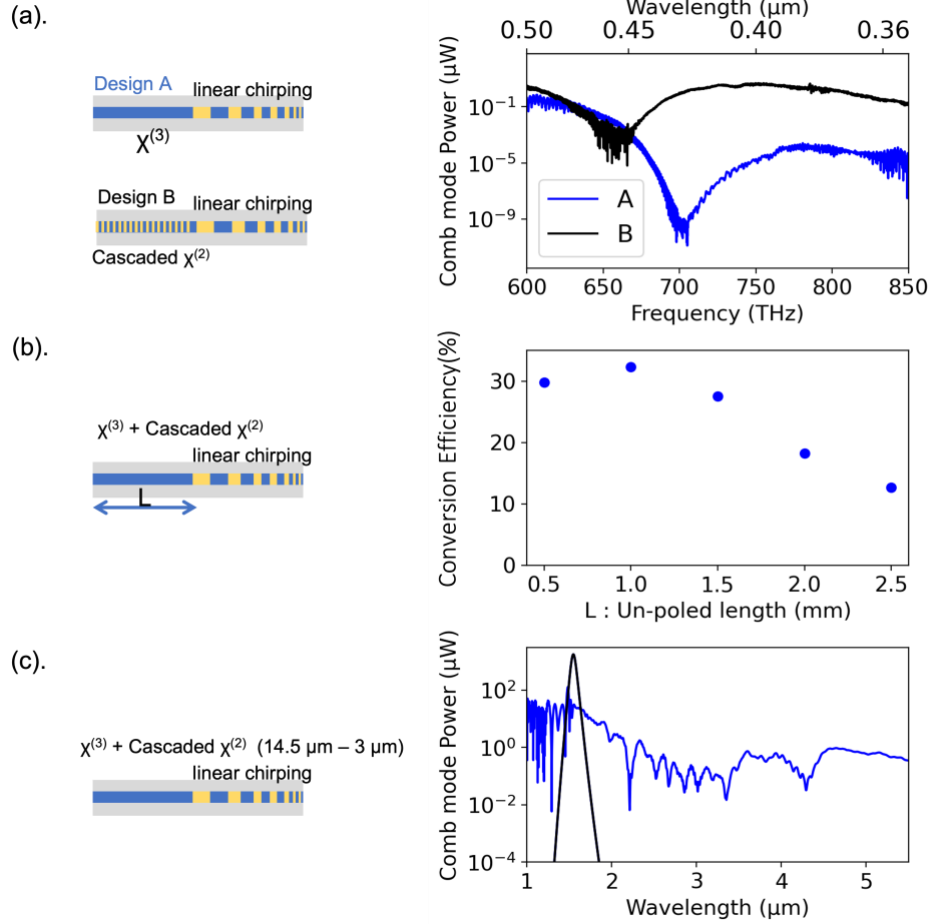
Supplementary Figure 1. (a) Calculated waveguide group velocity dispersion for the device used in this work. The dispersion for two waveguides with width of $w=1800$ nm and etched height of $h=350$ nm and $h=410$ nm on a 700 nm film. (b) Optical mode profiles and mode areas at the 4th (387.5 nm), 3rd (517 nm), and 2nd (775 nm) harmonics, as well as the fundamental (1550 nm), for the TE modes of the waveguide with $h=350$ nm.

Enhanced efficiency: A design to enhance the power in the spectral window of 350-500 nm is shown in Supplemental Fig. 2(a). Here, we compare the design employed in the main text ("Design A") with a design that enhances the visible and UV generation ("Design B"). In the new design, we propose a normal dispersion LN waveguide with fixed short poling pattern over the first segment. This period of $1.5 \mu\text{m}$ is chosen such that the 3rd and 4th harmonic spectra are enhanced and broadened with cascaded $\chi^{(2)}$ before the pulse enters the chirped poling segment. Figure 2(a) compares both designs, and "Design B" shows a theoretical improvement in power across 350-500 nm by more than 4 orders of magnitude with

only 30 pJ pump pulse energy. In this case, total conversion efficiency from 1550 nm to the 350-500 nm region is 15.9%.

In Fig. 5 of the main text we observe that the $\chi^{(3)}$ spectral broadening of the 1550 nm input pulse happens in the first few-hundred microns of propagation in the unpoled waveguide. Along with this spectral broadening, the pulse spreads in time and the peak power is decreased, which leads to lower efficiency in the nonlinear conversion. This observation leads us to investigate the impact of changing the length of the unpoled region, L , of the waveguide. (Note that $L = 3$ mm for the actual device described in the main text). Supplemental Fig 2(b) highlights the variation of conversion efficiency with L from the 1550 nm pump into a window covering 350-490 nm. Here we observe that for $L = 1$ mm a theoretical conversion efficiency of greater than 30% is possible. This type of analysis shows that further waveguide engineering can optimize the very-efficient projection of the 1550 nm light into specific spectral bands.

Infrared generation: Supplemental Fig. 2(c) shows a waveguide design that can lead to mid infrared (mid-IR) coverage. The height of the LN waveguide is 400 nm on a 710 nm film of LN on top of SiO₂ substrate. The length of waveguide is 6 mm, including a 5 mm unpoled segment, followed by a 1 mm segment with linearly chirped poling (3 μ m to 14.5 μ m). The waveguide dispersion is anomalous which enables soliton self-compression to increase the peak power and generate the desired bandwidth. The gap-free mid-IR coverage is generated with intrapulse difference frequency generation when the 50 pJ pump pulse propagates in the LN waveguide. Our model does not yet include the material absorption in the mid-IR in LN and thermal SiO₂ layers, but we see the potential to generate spectra across mid-IR with a sapphire substrate or fully air clad (suspended) waveguides.



Supplementary Figure 2. (a) Optimized wavelength coverage by design. Given a fixed pump energy of 30 pJ, the wavelength coverage produced by “Design B” shows a theoretical improvement in power in the UV spectral region by more than 4 orders of magnitude when compared to the original “Design A”. (b) Impact of input unpoled waveguide length L on the conversion efficiency from 1550 nm into the band spanning 350-490 nm. (c) Simulated anomalous dispersion waveguides with linear chirped poling pattern. The simulated spectra extends from 1 μm to beyond 5 μm (blue line) with a 5 mm long unpoled region that is followed by a 1 mm poled waveguide. The etch height is $h = 420$ nm and the width is $w = 1200$ nm. The simulation assumes a 50 fs and 50 pJ pump pulse (black line)